Mem. S.A.It. Suppl. Vol. 26, 19
© SAIt 2014

**Memorie** della
**Supplementi**

# New phase-magnitude curves for six Main Belt asteroids, fit of different photometric systems and calibration of the albedo - photometry relation

S. Caminiti[1,2], A. Carbognani[2], and A. Cellino[3]

[1] Università degli studi di Pavia, Dipartimento di Fisica, Via Bassi 6, 27100 Pavia, Italy
[2] Astronomical Observatory of the Autonomous Region of the Aosta Valley (OAVdA), Lignan 39, 11020 Nus, Aosta, Italy, e-mail: `albino.carbognani@gmail.com`
[3] INAF - Torino Astrophysical Observatory (INAF-OATo), Strada Osservatorio 20, 10025, Pino Torinese, Torino, Italy

**Abstract.** Preliminary results of photometric observations of eleven selected Main Belt asteroids are presented. The phase curves of these objects, which have values of geometric albedo well determined from stellar occultations or from WISE thermal IR measurements, increase the still small data-base of well-determined phase curves and can be used for a better calibration of the new photometric system ($H$, $G_1$, $G_2$) recently adopted by the IAU, as well as of other photometric systems used in the past. The new data are also useful for a more reliable determination of a proposed relationship between the slope of the linear part of the phase curve and the geometric albedo of the objects.

**Key words.** Minor planets – asteroids: phase curve, albedo

## 1. Introduction

The phase - magnitude curve (hereinafter, simply phase curve) of an asteroid describes the variation of brightness (normalized at unit distance from Sun and observer) as a function of phase angle. The phase angle is defined as the arc subtended by the directions to the observer and to the Sun as measured from the observed body. It is well known that asteroids exhibit the so-called opposition effect, namely a nonlinear brightening at small phase angles, generally below 7°. At larger phase angles the brightness tends to decrease linearly (Gehrels 1956).

Our observation program was aimed at obtaining accurate phase curves for a sample of selected asteroids, focusing on objects for which the geometric albedo seems to be well determined, based on accurate determinations of their sizes by means of star occultation measurements or thermal radiometry observations by the WISE (Wide-field Infrared Survey Explorer) satellite, (Shevchenko & Tedesco 2006; Pravec et al. 2012). For each asteroid in our observing program, we obtained a maximum possible number of lightcurves at different phase angles, as allowed by weather conditions and available telescope time. Of course, all data were taken for each object at the same apparition, so they all correspond for each object to a unique value of the aspect angle.

**Table 1.** The observed asteroids with rotation periods, geometric albedos, opposition date, minimum phase angle and number of lightcurves.

| Asteroid | Rotation period (h) | $p_v$ | Date Opp. | $\alpha_{min}$ (°) | LN |
|---|---|---|---|---|---|
| 236 Honoria | 12.333 | 0.127 | 2012-09-21 | 0.9 | 9 |
| 313 Chaldaea | 08.392 | 0.052 | 2012-09-22 | 0.3 | 6 |
| 522 Helga | 08.129 | 0.039 | 2012-10-02 | 1.8 | 7 |
| 085 Io | 06.875 | 0.067 | 2012-10-11 | 0.9 | 8 |
| 208 Lacrimosa | 14.085 | 0.269 | 2012-11-11 | 0.7 | 8 |
| 306 Unitas | 08.736 | 0.211 | 2012-11-11 | 5.2 | 7 |
| 135 Herta | 08.403 | 0.144 | 2012-12-10 | 1.5 | 3 |
| 338 Bubrosa | 04.608 | 0.177 | 2012-12-11 | 1.5 | 6 |
| 308 Polyxo | 12.032 | 0.048 | 2012-12-17 | 2.3 | 5 |
| 925 Alphonsina | 07.880 | 0.279 | 2012-12-29 | 5.4 | 6 |
| 444 Gyptis | 06.214 | 0.049 | 2013-01-03 | 5.3 | 7 |

**Table 2.** Root mean square in mag for the systems $HG$, $HG_1G_2$ and the Shevchenko model, with the numerical value of the constants.

| Ast. | $rms_{HG}$ | $rms_{HG_1G_2}$ | $rms_{Shev.}$ | $H$ | $G$ | $H$ | $G_1$ | $G_2$ | $V(1,0)$ | $b$ |
|---|---|---|---|---|---|---|---|---|---|---|
| 236 | 0.048 | 0.022 | 0.033 | 8.03 | 0.12 | 7.81 | +0.08 | 0.35 | 8.57 | 0.026 |
| 313 | 0.047 | 0.039 | 0.036 | 8.87 | 0.19 | 8.84 | +0.33 | 0.34 | 9.13 | 0.037 |
| 522 | 0.030 | 0.028 | 0.026 | 8.99 | 0.13 | 8.95 | +0.36 | 0.28 | 9.28 | 0.040 |
| 085 | 0.022 | 0.015 | 0.009 | 7.53 | 0.09 | 7.39 | +0.20 | 0.31 | 7.95 | 0.035 |
| 208 | 0.089 | 0.074 | 0.063 | 9.19 | 0.29 | 8.99 | -0.08 | 0.53 | 9.73 | 0.015 |
| 306 | 0.046 | 0.034 | 0.036 | 8.79 | 0.29 | 8.19 | -0.05 | 0.34 | 9.57 | 0.010 |
| $\overline{rms}$ | 0.05 ± 0.02 | 0.03 ± 0.02 | 0.03 ± 0.02 | | | | | | | |

In producing our phase curves, the magnitude was always taken for each object at either the maximum or minimum of the lightcurve (the one which turned out to be best determined for the set of available lightcurves of each object), to avoid introducing noise due lightcurve amplitude effects.

The primary purpose of our work was certainly to increase the database of available phase curves of good quality. In particular, such data are needed to achieve a better calibration of the new photometric system ($H$, $G_1$, $G_2$), or ($H$, $G_{12}$) (Muinonen et al. 2010) recently adopted at the 2012 IAU General Assembly. In addition, the availability of new phase curves is also important to better check the validity and improve the calibration of a possible relationship that has been proposed to exist between the slope of the linear part of asteroid phase curves and the geometric albedo of the objects (Shevchenko 1997; Belskaya & Shevchenko 2000).

This can be very important for the scientific exploitation of the photometric data which will be recorded by the Gaia mission of ESA (European Space Agency), whose launch is now imminent (autumn 2013). Gaia will get sparse photometric data for thousands of asteroids. By inversion of Gaia photometric data, it will be possible to derive the slope of the phase curve in a range of phase angles where the trend is essentially linear, therefore it is in principle tempting the possibility to use these data to derive also an estimate of the albedo of these objects.

## 2. Choice of the targets

In choosing our targets, we were driven not only by availability of a presumably reliable albedo value from the lists in (Shevchenko & Tedesco 2006) and (Pravec et al. 2012), but we were forced to constraints on the epoch of their next opposition (to be between September and December 2012), the minimum reachable phase angle (if possible less than 2°) and the rotational period (short period being preferred for an easier and faster determination of the lightcurve). The rotation periods for the observed asteroids were already known and have been taken from the Asteroid Light Curve Data Base, or ALCDB (Warner et al. 2009).

Some asteroids with minimum phase angle greater than 5° were also added to the program, since they satisfied out criteria above, and we were interested to get more data for the study of the linear part of the phase curve. The list of our targets is shown in Table 1.

## 3. Instruments and reduction procedures

Observations were performed between September 2012 and February 2013 at OAVdA (Astronomical Observatory of the Autonomous Region of Aosta Valley), located in north-western Italian Alps (Calcidese et al. 2012). We used a 810mm f/7.9 modified Ritchey-Chrétien reflector on a fork equatorial mount combined with a back illuminated CCD camera, 2048 × 2048 square pixel with size of 15 micron. The CCD was used in binning 2 × 2 with a FOV (Field Of View) of 16.5 × 16.5 arcmin. The telescope is equipped with a filter wheel with B, V, R, I and C standard filters.

The work at the telescope was divided in two steps:

- Asteroid photometric observations in V and R band.
- Calibration of the observed FOVs with Landolt fields in V and R band (all–sky photometry).

We processed our data in order to obtain a Fourier fit of each asteroid lightcurve and we merged together whenever possible different nights of observation. In this way we obtained complete lightcurves for each asteroid at different values of phase angle. Then, we computed the true V and R magnitudes of the adopted comparison stars by using some Landolt calibration fields (see next section). This was followed by a calibration of the asteroid lightcurves using properly reduced magnitude and a final fit of the lightcurves' Fourier models to derive the magnitude of the max and the min values (Warner at al. 2010). These magnitude data, properly reduced to 1 UA from Earth and Sun, were used to obtain a best fit (in the sense of least squares), of the obtained phase curves. In so doing, we used both the older $H, G$ and the newly adopted $H, G_1, G_2$ photometric systems, as well as the Shevchenko model.

## 4. The Landolt field calibration

Whenever the night was photometric, we proceeded with the Landolt field imaging in V and R for a correct measurement of the real magnitude of the comparison stars selected for each night of observation. We took some images of various Landolt fields at various air masses to calibrate the atmospheric extinction (Harris et al. 1981).

We measured the V and R instrumental magnitude for each Landolt star (taking the average of 5 images per filter). From the instrumental magnitude, a four parameters atmospheric model was fitted by the following equations:

$$V - v = -[k_{1v} + k_{2v}(V - R)]X + c_v(V - R) + V_0 \quad (1)$$

$$R - r = -[k_{1r} + k_{2r}(V - R)]X + c_r(V - R) + R_0 \quad (2)$$

where:

- $k_1$ is the atmospheric extinction
- $k_2$ is the color extinction
- $c$ is the color correction
- $R_0$ and $V_0$ are the zero point
- $V, R$ and $V-R$ are the tabulated magnitudes
- $v$ and $r$ are the instrumental magnitudes
- $X$ is the air-mass

After finding the various parameters of the atmospheric model, it was possible to calculate

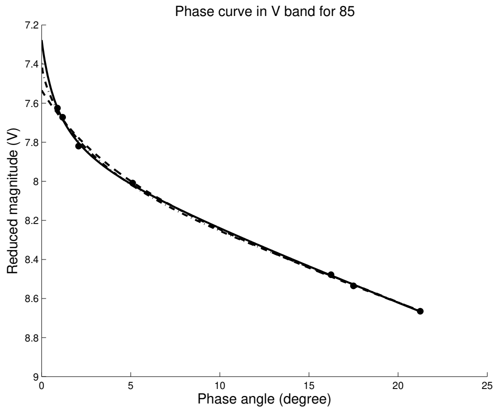


**Fig. 1.** Phase curve in V band for 85 Io. For the meaning of the different fitting curves, see the text.

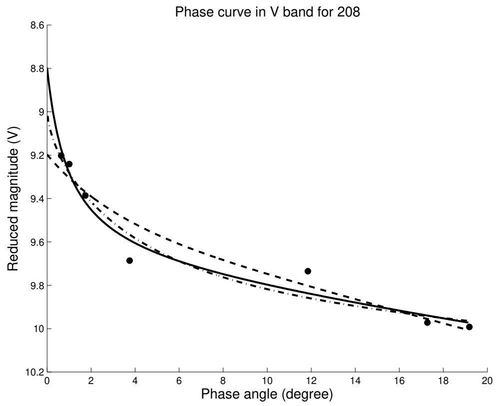


**Fig. 2.** Phase curve in V band for 208 Lacrimosa.

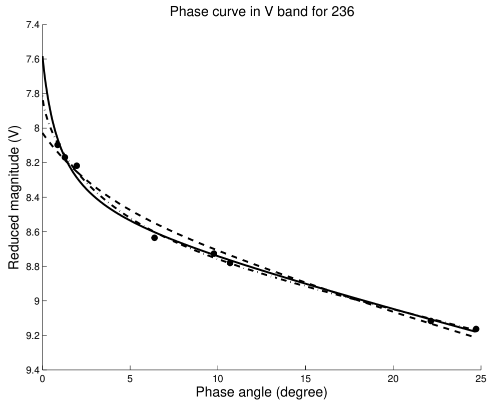


**Fig. 3.** Phase curve in V band for 236 Honoria.

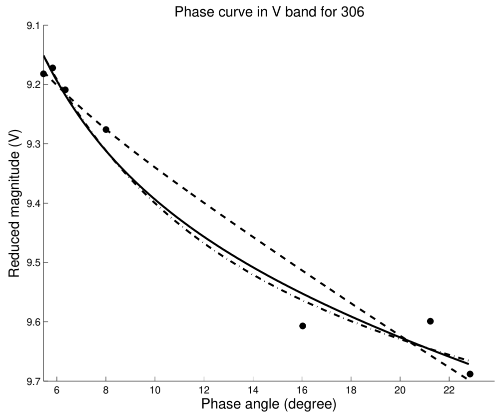


**Fig. 4.** Phase curve in V band for 306 Unitas.

the true V and R magnitude of the comparison stars by taking some images, in the same night, of the FOV in which asteroids were located, measuring the comparison stars instrumental magnitudes according to the atmospheric model.

To calculate the true mag of the asteroid we assumed that the V-R of the comparison stars are about equal (within few hundredths of mag) to the V-R of the asteroid (for this purpose we used only solar-type comparison stars). From the previous atmospheric model we obtain (*a*=asteroid, *c*=comparison star):

$$V_c - V_a = v_c - v_a \quad (3)$$

$$R_c - R_a = r_c - r_a \quad (4)$$

From these equations it is possible to calculate the true mag of the asteroid.

## 5. The results

The phase curves for six objects of our sample are shown in the Figs. 1, 2, 3, 4, 5 and 6. For the remaining five targets of our program (see Table 1), observations are still being reduced, and definitive results with more phase curves will be published in a separate paper.

The phase curves shown here are always built using the maximum brightness of the asteroid lightcurve. In all the figures, the dashed-dashed line corresponds to the best fit obtained using the $H, G$ photometric system. Dot-dashed curves show the fit corresponding to

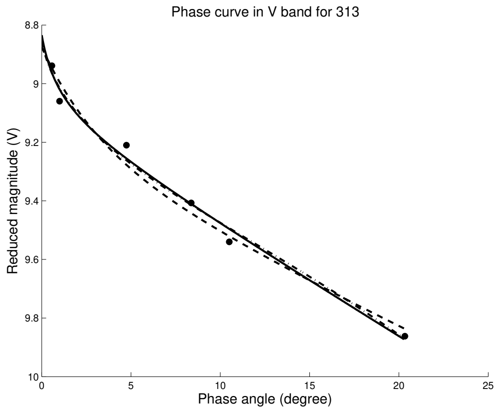


**Fig. 5.** Phase curve in V band for 313 Chaldaea.

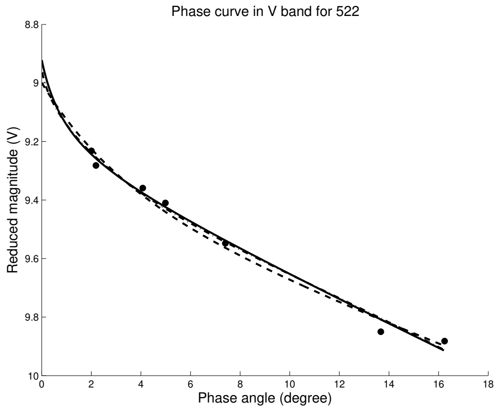


**Fig. 6.** Phase curve in V band for 522 Helga.

the new $H, G_1$, $G_2$ system. The continuous lines correspond to the fits of the Shevchenko model.

It is easy to see that the residual rms (root mean square) obtained using the $H$, $G_1$, $G_2$ and the Shevchenko photometric systems are in general significantly lower than the rms obtained using the $H, G$ system, as quantitatively shown in Table 2. One should also note, by a visual inspection of the figures, how important are the differences among the values of absolute magnitude (the value of the curves at zero phase angle) when different photometric systems are used. In particular, the absolute magnitudes obtained using the $H, G$ systems tend to be seriously fainter in one half of the cases shown in our figures (see Table 2).

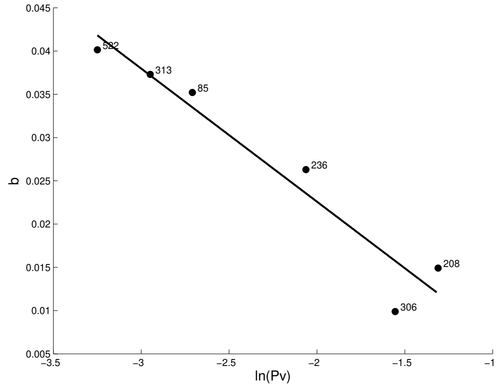


**Fig. 7.** Linear relationship between the slope of the linear part of the phase curve and the log of the geometric albedo in the Shevchenko model.

Albeit with the limited data now available, we have analyzed a possible linear correlation between the slope of the linear part of the phase curve and the log of the geometric albedo (Belskaya & Shevchenko 2000). We obtain the following linear relation:

$$b = -0.0082 - 0.0154 \cdot \ln(p_v) \tag{5}$$

that is not too different from that found by (Shevchenko 1997). The correlation coefficient is 0.96, a very good value, but it is clear that more data are needed before drawing definitive conclusions.

## 6. Conclusions

We have obtained new phase curves in the range $0° - 30°$ for a sample of eleven Main Belt asteroids, and we obtained best fits corresponding to the $H, G$, $HG_1G_2$, and Shevchenko photometric systems for six of them. The rms appear to be significantly worse using $H, G$. A possible relation between the linear part of the phase curves and the asteroids geometric albedo is not ruled out by our observations, and is confirmed to be potentially important for the imminent Gaia mission. Additional phase curves will be added in the months to come and the full results of our program, with the numerical data, will be published soon. If you are interested to numerical data for the six reduced phase curves of this paper send an e-mail to the corresponding author.

## References

Belskaya, I. N., & Shevchenko, V. G. 2000, Icarus 147, 94
Calcidese, P., et al. 2012, Mem. SAIt Suppl., 19, 368
Gehrels, T. 1956, AJ 123, 331
Harris, W. E., Fitzgerald, M., & Cameron Reed, B. 1981, PASP, 93, 507
Muinonen, K., et al. 2010, Icarus, 209, 542
Pravec, P., et al. 2012, Icarus, 221, 365
Shevchenko, V. G. 1997, Solar System Research, 31, 219
Shevchenko, V. G., & Tedesco, E. F. 2006, Icarus, 184, 211
Warner, B., et al. 2009, Icarus, 202, 134
Warner, B.D., Foote, J., Buchheim, R. 2010, 29th Symposium on Telescope Science (The Society for Astronomical Science, Rancho Cucamonga, CA)